School of Mathematics, Meteorology
and Physics

Department of Mathematics

Preprint MPS_2010-05

18 March 2010

Numerical estimation of coercivity constants for boundary integral operators in acoustic scattering

by

T. Betcke and E.A. Spence

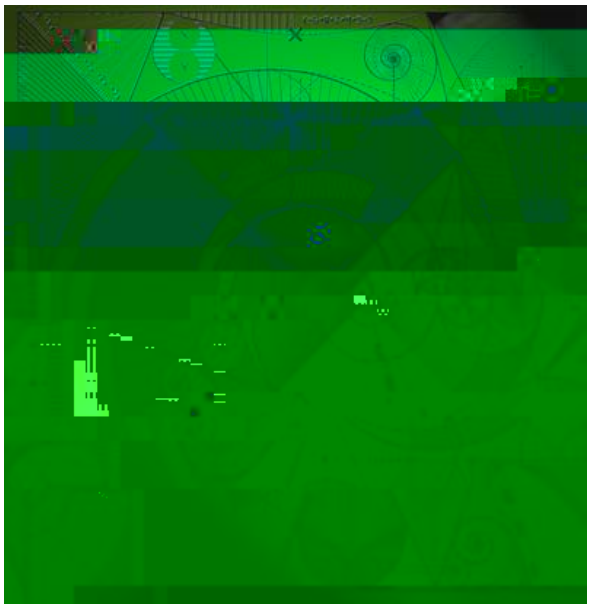

NUMERICAL ESTIMATION OF COERCIVITY CONSTANTS FOR BOUNDARY INTEGRAL OPERATORS IN ACOUSTIC SCATTERING

T. BETCKE AND E.A. SPENCE[y]

Abstract. Coercivity is an important concept for proving existence and uniqueness of solutions to variational problems in Hilbert spaces. But, while the existence of coercivity estimates is well known for many variational problems arising from partial di erential equations, it is still an open problem in the context of boundary integral operators arising from acoustic scattering problems, where rigorous coercivity results have so far only been established for combined integral operators on the unit circle and sphere. The main motivation for investigating coercivity in this context is that it has the potential to give error estimates for the Galerkin method which are explicit in the wavenumber k. One way to interpret coercivity is by considering the numerical range of the operator. The numerical range is a well established tool in spectral theory and algorithms exist to approximate the numerical range of nite dimensional matrices. We can therefore use Galerkin projections of the boundary integral operators to approximate the numerical range of the original operator. We prove convergence estimates for the numerical range of Galerkin projections of a general bounded linear operator on a Hilbert space to justify this approach. By computing the numerical range of the combined integral operator in acoustic scattering for several interesting convex, nonconvex, smooth and polygonal domains, we numerically study coercivity estimates for varying wavenumbers. Surprisingly, it turns out that for many domains a coercivity result seems to hold independently of the wavenumber or with only a mild dependence on it. Finally, we consider a trapping domain, for which there exist resonances (also called scattering poles) very close to the real line, to demonstrate that coercivity for a certain wavenumber k seems to be strongly dependent on the distance to the nearest resonance.

Key words. numerical range, coercivity, boundary integral operators

AMS subject classi cations. 45P05, 47A12, 65R20,

1. Introduction.

Let H be a Hilbert space and $t : H \times H \to \mathbb{C}$ a sesquilinear form on H. A standard variational problem is to nd $u \in H$ such that

$$t(u; v) = f(v); \quad \forall v \in H \tag{1.1}$$

for a given $f \in H^0$, the dual space of H.

where $u = u_{inc} + u_s$ is the total field, u_{inc} is a solution of (1.5) in a neighborhood of , such as an incident plane wave, u_s is the scattered field, and r is the radial coordinate. With the standard free-space Green's function defined as

$$(x;y) = \frac{i}{4}H_0^{(1)}(kjx \quad yj);\ d = 2; \qquad (x;y) = \frac{e^{ikjx \quad yj}}{4\ jx \quad yj};\ d = 3;$$

for $x;y\ 2\ \mathrm{R}^d;x \neq y$, the solution u is given by

$$u(x) = u_{inc}(x) \qquad (x;y)u_n(y)ds(y); \quad x\ 2\ \mathrm{R}^d\bar{n};$$

where u_n is the outward pointing normal derivative of u. To compute u_n one can solve the boundary integral equation

$$A_{k;}\ u_n = 2\frac{@u_{inc}}{@n} \quad 2i\ u_{inc} \tag{1.8}$$

with

$$A_{k;} := I + K^0 \quad i\ S; \tag{1.9}$$

where $\ 2\ \mathrm{R}nf0g$, I is the identity, and K^0 and S are defined by

$$K^0u(x) := 2 \qquad \frac{@\ (x;y)}{@n(x)}u(y)ds(y); \quad Su(x) := 2 \qquad (x;y)u(y)ds(y); \quad x\ 2\ :$$

Here, $n(x)$ is the outward pointing unit normal at . The corresponding sesquilinear form is defined as $a_{k;}\ (u;v) := hA_{k;}\ u;vi$, with $hu;vi := \quad u(y)$

A rst result on the coercivity of $a(\ ;\ )$ was given in [18], where it was shown that with the unit circle (in 2-d) and the unit sphere (in 3-d) $a(\ ;\ )$ is coercive for su ciently large k with 1. However, the question of coercivity and of k dependence of is still unanswered for more complicated domains. In Section 2 we give an overview of existing coercivity results. To numerically estimate the coercivity constant on more complicated domains we use the close connection between coercivity and the numerical range of the operator A. The numerical range is de ned as the set of all values $\langle Au;u\rangle$ in the complex plane with $u \in L^2(\ )$, $\|u\| = 1$. It holds that $a(\ ;\ )$ is coercive if and only if 0 is not in the closure of the numerical range. Hence, we can determine coercivity by computing the numerical range of the operator A, which is a well studied problem in the numerical linear algebra literature for matrices acting on $\mathbb{C}^n$. In Section 3 we describe some key properties of the numerical range, and in Section 4.1 we review a well known simple algorithm for computing the numerical range of an operator. Since in practice we need to work with Galerkin discretizations of $a(\ ;\ )$ in Section 4.2, we give convergence estimates of the numerical range based on Galerkin discretizations with standard piecewise constant boundary element discretizations. In Section 5 we demonstrate numerically the convergence of the numerical range and use the numerical range computations to give numerical estimates of the coercivity constant for several interesting polygonal and smooth domains in two dimensions. We summarize our results and give conjectures about the coercivity constant in Section 6.

2. A summary of stability results for boundary integral operators in acoustic scattering. In this section we summarize the known continuity and coercivity results about the operator A, namely whether the inequalities (1.2) and (1.3) hold, and if so, how the constants C and depend on k. We note that these results also apply to the related operator:

$$A'_{k;} := I + K \quad i\ S \tag{2.1}$$

where K is the double layer potential

$$Ku(x) := 2 \int \frac{@\ (x;y)}{@n(y)} u(y)ds(y); \quad x\ 2\ :$$

This operator appears in the classic indirect boundary integral formulation due to Brakhage and Werner [8], Leis [28] and Panic [33]. (\Indirect" refers to the fact that this integral operator does not arise from Green's integral representation, whereas the so-called \direct" integral operator (1.9) does.) The operator $A'_{k;}$ is the adjoint of $A_{k;}$ with respect to the real inner product $\langle u;v\rangle_R := \int u(y)v(y)ds(y)$. Thus

$$\|A_{k;}\|_{k} = \|A'_{k;}\|_{k;}$$

where the norm is that induced by the standard L^2-inner product, and if the inequalities (1.2), (1.3) hold for $A_{k;}$ then they also hold for $A'_{k;}$ with the same $C;$.

Much less is known about coercivity (1.3) than continuity (1.2), so we discuss coercivity rst. We then include a brief discussion of continuity results, for more comprehensive treatments see [13, 12]. In this section we will use the notation $D \ . \ E$ where $D=E$ is less than a constant which is independent of k.

2.1. Coercivity. The only domains for which coercivity is completely understood is the circle (in 2-d) and sphere (in 3-d); this is because the operator A acts diagonally in the basis of trigonometric polynomials or spherical harmonics in 2 and 3-d respectively. For the circle, Dom nguez, Graham and Smyshylaev [18] showed that for the case $= k$ coercivity holds for all su ciently large k, with

$$1;$$

and for the sphere they proved

$$1 \quad O(k^{\ 2=3}):$$

These di cult proofs relied on bounding below the eigenvalues of A, which are combinations of Bessel functions, uniformly in argument and order.

Although nothing is known directly about the coercivity constant for domains other than the circle/sphere, results on the norm of the inverse of A can be used to deduce information about using the fact that if A is coercive then

$$\frac{1}{kA^{-1}k}.$$

This follows from (1.3) using Cauchy-Schwartz. Chandler-Wilde, Graham, Langdon and Linder [13] proved that if a part of is C^1 then

$$kA^{-1}k \quad 1 \tag{2.2}$$

and hence

$$1. \tag{2.3}$$

Thus the bound obtained for for the circle in [18] is sharp. (2.2) follows from the fact that S and K are smoothing operators on smooth parts of . In the same paper the authors constructed an example of a non-convex, non-starlike \trapping" domain in 2-d for which there exists an increasing sequence k_n where $kA^{-1}k$ grows as k_n increases. Indeed, for this domain, when $= k$,

$$kA^{-1}k \ \& \ k_n^{9=10} \tag{2.4}$$

where B is independent of k. It is not known whether

for su ciently large k

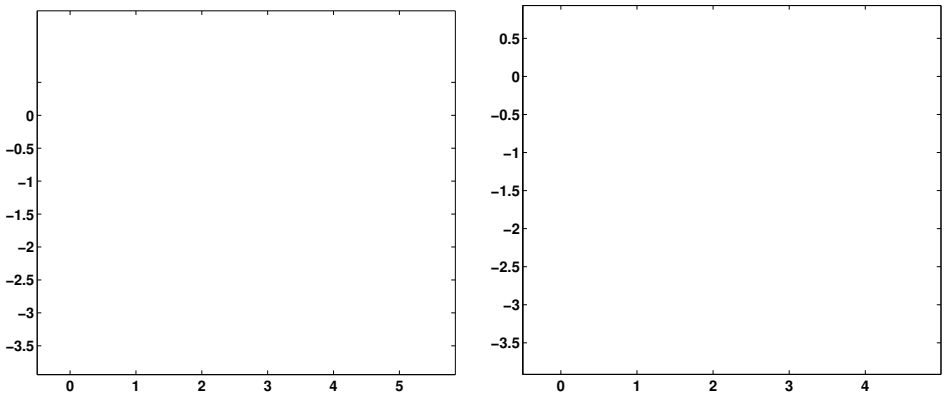

Fig. 3.1: Eigenvalues and boundary of the numerical range of the boundary integral operator $A_{k;}$ on the unit circle (left plot) and on the equilateral triangle with side length 1 (right plot) for $k =$ $= 50$.

Lemma 3.5. *If* *is the boundary of the unit circle (in 2-d) or the unit sphere (in 3-d) then* $A_{k;}$

Proposition 3.6. *Let T be a bounded linear operator. The following statements are equivalent:*

(i) $0 \in$

and right bound for the numerical range $W(e^{i\theta} T)$ obtained as in (4.1). We have the following algorithm to compute the coercivity constant γ.

Input: Bounded linear operator T, Number of approximating points N
Output: 0 or lower bound for coercivity constant

```
W := ℂ; angles := { j/N ; j = 0, ..., N − 1 };
foreach θ ∈ angles do
    Compute h^(m), h^(M);
    W := W ∩ e^{−iθ} { z ∈ ℂ : h^(m) ≤ Re{z} ≤ h^(M) };
end
if 0 ∉ W then
    return γ := d(0, W);
else
    γ := 0;
end
return γ;
```

Algorithm 1: Computation of coercivity constant

Algorithm 11 computeg3811

as Galerkin discretisation and the variational characterisation of the numerical range it follows immediately that

$$W(T^{(h)}) = \{\langle Tu, u\rangle : u \in V^{(h)},\ \|u\| = 1\} \subset W(T).$$

In this section we will use the notation $d(X,Y) := \inf\{|x - y| : x \in X,\ y \in Y\}$ for the distance of two sets. Correspondingly, $d(x,Y) := d(\{x\},Y)$ is the distance of a single point x to the set Y. For the analysis we need the following perturbation Lemma.

Lemma 4.1. *Let $z \in W(T)$ with associated $u \in H$, $\|u\| = 1$, such that $z = \langle Tu, u\rangle$. Let $0 < \varepsilon < 1$ and choose $\hat{u} \in H$ with $\|u - \hat{u}\| \le \varepsilon$. Then*

$$z \in \frac{\langle T\hat{u}, \hat{u}\rangle}{\langle \hat{u}, \hat{u}\rangle} + \overline{B}_{8\|T\|\varepsilon}(0);$$

Proof. Let $f = u - \hat{u}$. Then $\|f\| \le \varepsilon$. We have

$$z = \langle T(\hat{u} + f), \hat{u} + f\rangle$$

and therefore

$$|z - \langle T\hat{u}, \hat{u}\rangle| \le 2\|T\|\|\hat{u}\|\|f\| + \|T\|\|f\|^2. \tag{4.2}$$

We now estimate

$$\begin{aligned} |z - \langle T\hat{u}, \hat{u}\rangle| &\le \left|z - \frac{\langle T\hat{u}, \hat{u}\rangle}{\langle \hat{u}, \hat{u}\rangle}\right| + \left|\langle T\hat{u}, \hat{u}\rangle - \frac{\langle T\hat{u}, \hat{u}\rangle}{\langle \hat{u}, \hat{u}\rangle}\right| \\ &\le \left|z - \frac{\langle T\hat{u}, \hat{u}\rangle}{\langle \hat{u}, \hat{u}\rangle}\right| + \|T\|\,|1 - \|\hat{u}\|^2|. \end{aligned} \tag{4.3}$$

Combining this with (4.2) and using $|1 - \|\hat{u}\|^2| \le 2\|f\| + \|f\|^2$ gives

$$z \in \frac{\langle T\hat{u}, \hat{u}\rangle}{\langle \hat{u}, \hat{u}\rangle} + \overline{B}_{2\|T\|\|f\|[\|\hat{u}\| + \|f\| + 1]}.$$

With $\|\hat{u}\| \le \|u\| + \|f\| = 1 + \|f\|$ we have

$$z \in \frac{\langle T\hat{u}, \hat{u}\rangle}{\langle \hat{u}, \hat{u}\rangle} + \overline{B}_{2\|T\|\|f\|[2 + 2\|f\|]} \subset \overline{B}_{8\|T\|\varepsilon}$$

since $\|f\| \le \varepsilon \le 1$. □

We can now give a first convergence result. In order to state it we define the set $W_\varepsilon(T) := \{z$

represented in H ( ) *for some* < 1

The key point about equation (4.7) is that each term on the right hand side is the product of two errors in Galerkin approximations, thus the Galerkin approximation to the functional $\langle u; Xu \rangle$ converges faster than $\|u - u^{(h)}\|$ { this is an example of superconvergence. Another example of Galerkin approximations of functionals exhibiting superconvergence is given in [34].

Using Lemma 4.5 instead of Lemma 4.1 we can now prove a re ned version of Theorem 4.4 for the numerical range of self-adjoint operators.

Theorem 4.7. *Let be a Lipschitz domain with boundary and* $X : L^2(\ ) \to L^2(\ )$ *a self-adjoint bounded linear operator which also maps* $H^1(\ )$ *to* $H^1(\ )$*. Denote by* $X^{(h)}$ *its Galerkin discretisation from a space* $V^{(h)} \subset L^2(\ )$

Proof. Splitting up $A_{k;}$ into A_H and A_S

Fig. 5.1: Convergence of the coercivity constant for a growing number of elements per wavelength on the unit circle for $k = 1$ with linear and quadratic basis functions.

the discretisation only lls parts of the exact numerical range, leading to an overestimation of the coercivity constant. The (up to plotting accuracy) correct numerical range was obtained by using piecewise quadratic basis functions together with exponential h-re nement towards corners. The lower right plot shows the approximate spectrum (black dots) and the boundary of the numerical range obtained with this strategy. The convergence of the coercivity constant $^{(h)}$ for the re ned discretisations is shown as the circle-dotted line in the upper left plot of Figure 5.2. N means here that approximately N elements per wavelength were used until a distance of $\frac{2}{Nk}$ away from the corner together with exponential h-re nement in the direct neighbourhood around the corner. This gives an accuracy of around 10^{-2} for $N = 10$. The best obtained value for the coercivity constant on the square is 0:318 using $N = 3000$. As comparison for $N = 10$ we obtain 0:329, a relative distance of less than 4% to the best value. On the plotting scale there is no signi cant di erence lacway 6(aen)28(w)7(erci0 l S Q BT /Fml S QBT 7(erc(the)-3(the)-298(corn123.848 0 Td [(J/Ft)]TJ1(th

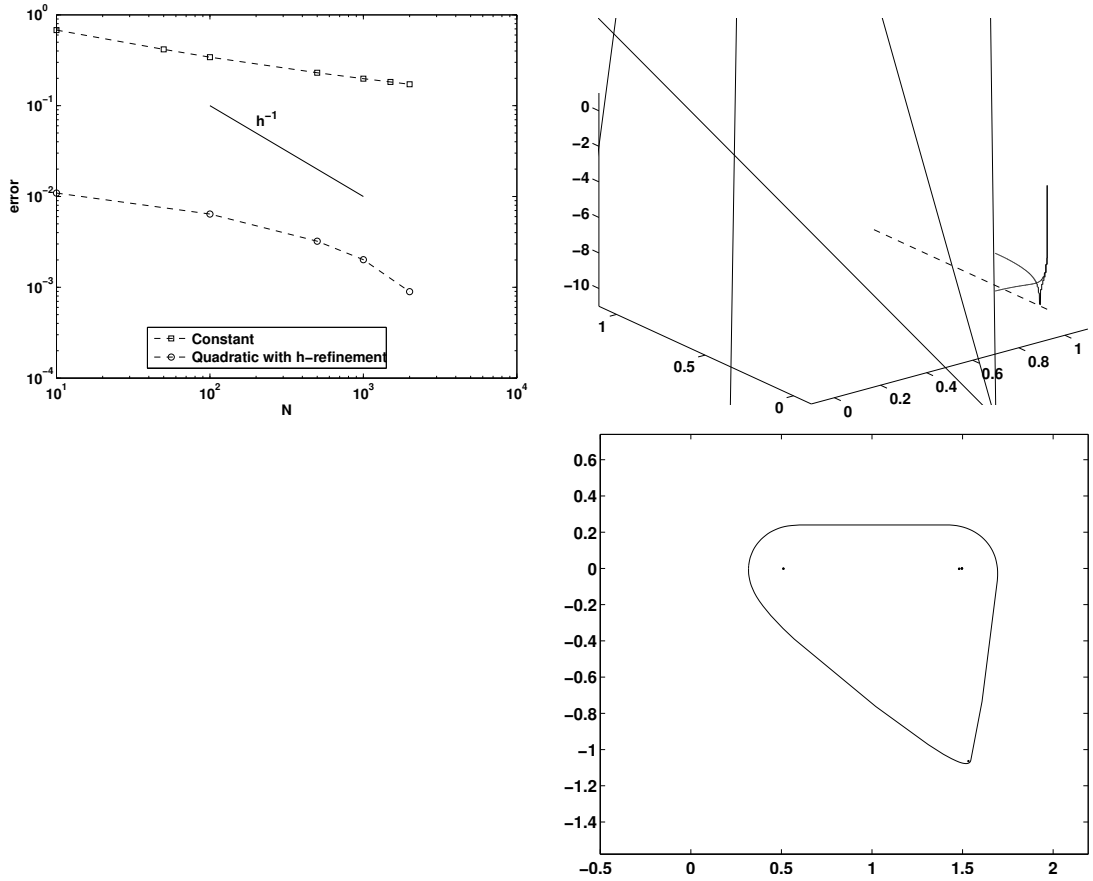

Fig. 5.2: Upper left:) Rate of convergence of $^{(h)}$ on the unit square. Upper right:) A function associated with a point of the numerical range close to 0:5 . Lower left:) Approximate numerical range using piecewise constant basis functions (solid line) against exact numerical range (dotted line). The dots show the eigenvalues of the Galerkin projection $A^{(h)}$. Lower right:) Approximation to exact numerical range and the spectrum of A on the square obtained by using piecewise quadratic basis functions and h-re nement towards corners of the square.

was roughly in the range of 12 to 20 hours for the largest matrix problems. Due to the cubic dependence of the computing time for the full matrix problems on the dimension of the matrices, doubling the number of elements leads to an additional factor 8 in time.

5.2.1. Smooth domains. For the unit circle coercivity was already shown for su ciently large k in [18]. Therefore, we are more interested for this domains in what happens as $k \to 0$. The corresponding values of the coercivity constant are given in the following table.

k	0.01	0.1	1	10
	0.01	0.57	1.00	1.00

For $k = 1$ and above the coercivity constant indeed seems to be 1. However, as $k \to 0$ the numerical range starts deteriorating into a line and it appears that also $\to 0$. This is consistent with the fact that the choice $= k$ is not optimal for small wavenumbers (see Section 2), and also with the fact that $A_0 = I + K_0^0$ is not invertible, and hence not coercive, on $L^2(\ )$ for any Lipschitz domain since it maps any L^2 function into one with zero mean and hence is not surjective [38]. However, if we $x = 1$, then for $k = 0{:}1$ and $k = 0{:}01$ we obtain that the coercivity constant is 1. Since the

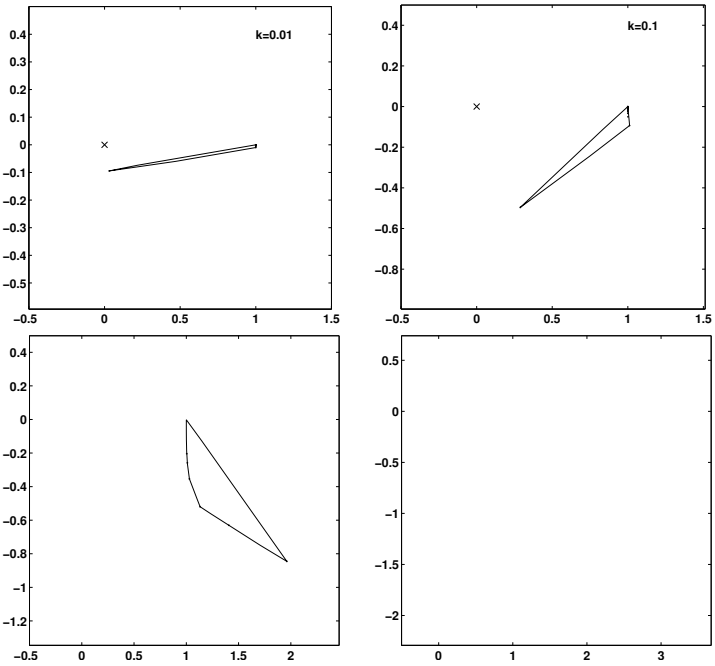

Fig. 5.3: The numerical range of A on the unit circle for $k = 0{:}01; 0{:}1; 1; 10$. The black dots are approximations to the spectral values of A.

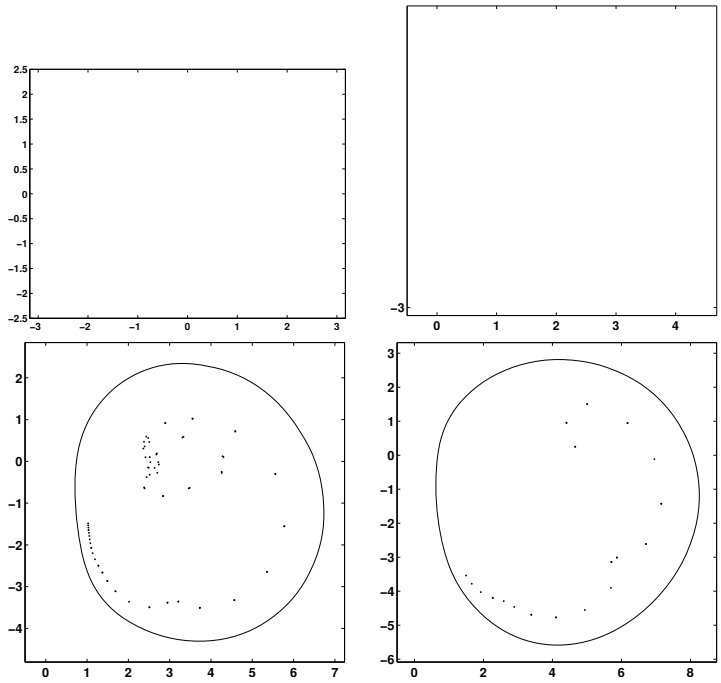

Fig. 5.5: An inverted ellipse and the associate numerical range of A for $k = 10; 50; 100$.

eigenvalues of A on the unit circle are explicitly known (see for example [18]) and the numerical range is just the convex hull of the spectrum in this case one may also approximate the coercivity constant for the unit circle directly without using a Galerkin discretization of the operator. Also, it is interesting to note that for growing k more and more eigenvalues cluster around the point 2 (see Figure 3.1). However, for each k there can only be a nite number of eigenvalues close to 2 since A on the unit circle is a compact perturbation of the identity and therefore the only accummulation point of the eigenvalues is 1.

The next domain is a kite shape. A parameterization of its boundary is given by $Z(t) = \cos t + 0.65 \cos 2t \quad 0.65 + 1.5i \sin t$, $t \in [0; 2\ ]$. The numerical range for $k = 10; 50; 100$ is shown in Figure 5.4. Again, as in the case of the unit circle there are more and more eigenvalues appearing close to 2 as k becomes larger. However, the main di erence between this domain and the circle is that the operator A is not normal since the numerical range is not just the convex hull of the eigenvalues. But interestingly we still have 1 for all three cases. Again, the coercivity constant seems to be independent of the wavenumber for su ciently large k. The size of the numerical range grows as k becomes larger. This is due to the norm bound (2.5) and the equivalence of the numerical radius and the norm of A in (3.4).

In the next example we show results for a domain, which like the kite is nonconvex and star-shaped but for which the coercivity constant of A shows a very di erent behaviour for growing k. It is an inverted ellipse de ned by $Z(t) = \frac{e^{it}}{1+\frac{1}{2}e^{2it}}$, $t \in [0; 2\ ]$. The inverted ellipse and the corresponding numerical range of A for $k = 10; 50;$

the inverted ellipse or whether ! 0 as k ! 1 (see also the discussion in Section 6).

5.2.2. Polygonal domains. We start with two simple convex polygons, namely the unit square and the equilateral triangle. For the unit square and $k = 1$ a plot of the numerical range was already shown in Figure 5.2. We now present results for growing k. Figure 5.6 shows the numerical range and approximations of the spectra for A on the square in the case of the wavenumbers $k = 10; 50; 100$. The lower right plot shows a comparison of the numerical range in all three cases. Again, due to (2.6) and (3.4) the size of the numerical range grows for growing k. For we obtain in all three cases the approximation 0:328. It is interesting to note that close to the origin for all three wavenumbers the boundary of the numerical range is almost identical (see the lower right plot of Figure 5.6). For $k = 1$ we computed a value of 0:318 using approximately 3000 elements per wavelength while here we used around 20 elements per wavelength. Hence, the value of for the higher wavenumbers has a relative distance of around 3% to the value for $k = 1$, which is likely due to the higher discretisation error (note that for 10 elements per wavelength we reported a value of 0.329 in Section 5.1).

As Figure 5.7 shows the operator A on the equilateral triangle has a very similar behaviour. Again, the computed coercivity constant does not seem to change in dependence on the wavenumber. For the three considered wavenumbers $k = 10; 50; 100$ we have 0:17.

The square and the triangle are both convex domains, and both exhibit numerical wavenumber independence of . To see that this feature is not restricted to convex polygonal domains consider the L-Shape in Figure 5.8. Again, the coercivity constant seems to be independent of the wavenumber with a value of 0:30. Figure 5.9 shows the results for a polygon which is not only non-convex, but is also non-star-shaped, and again the results are very similar to the other domains. In this example we have 0:30 for all three wavenumbers, which interestingly is, up to numerical accuracy, identical to the value for the L-Shape.

5.3. A trapping domain. Our last example is the trapping domain shown in Figure 5.10, so-called because the open cavity can \trap" high frequency waves. That is, we expect there to be asymptotically trapped modes of the PDE (1.5) in the cavity for large wavenumbers k that are multiples of 5 (since the width of the cavity is =5). This fact was used in [13] to show that for this domain $kA^{-1}k$ satis es (2.4) for k_n multiples of 5, and hence the operator A cannot be uniformly coercive for large k. Figure 5.11 shows the numerical range of A for this domain in the cases $k = 4; 5; 8; 10$. For $k = 4$ and $k = 8$ the operator A is coercive. But for $k = 5$ and $k = 10$ we lose coercivity. These numerical results seem to indiciate that the loss of coercivity is closely connected to the nonnormality of the operator: for all wavenumbers in Figure 5.11 the spectrum of A is in the right-half plane independent of whether the operator is coercive or not. This again suggests that spectral information is not su cient to understand coercivity. We now give a possible explanation for the loss of coercivity at $k = 5$ and $k = 10$ by considering resonances of the exterior scattering problem. A resonance (or scattering pole) can be de ned as a wavenumber k_{res}, for which there exists a sequence $u^{(n)}$ 2 L^2( ), $ku^{(n)}k$

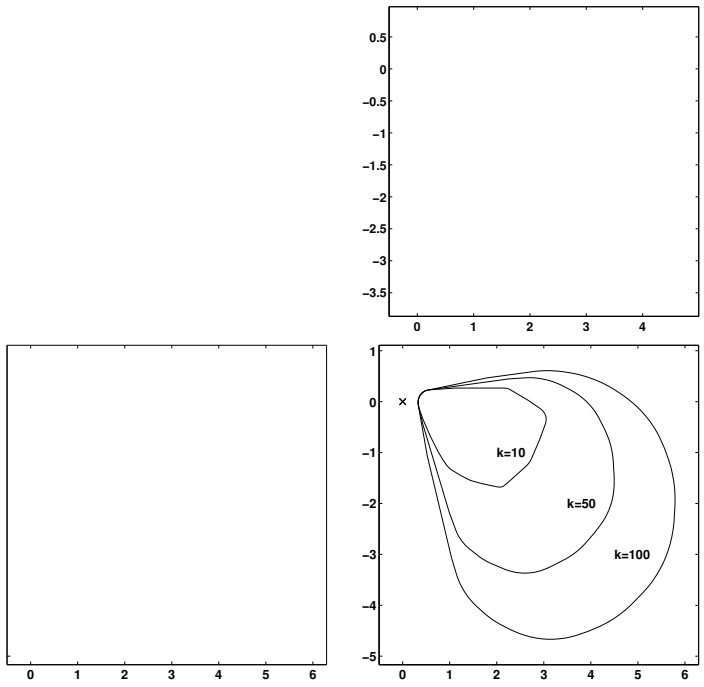

Fig. 5.6: The numerical range of A on the unit square for $k = 10; 50; 100$. The black dots are approximations to the spectral values of A. The lower right plot shows a comparison of the numerical ranges for the three di erent wavenumbers.

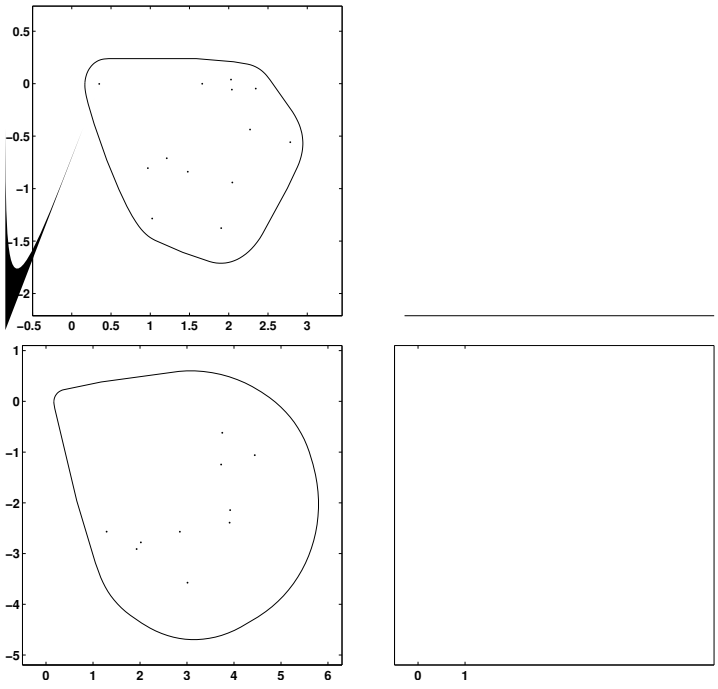

Fig. 5.7: The numerical range of A on the equilateral triangle with sides of unit length for $k = 10; 50; 100$.

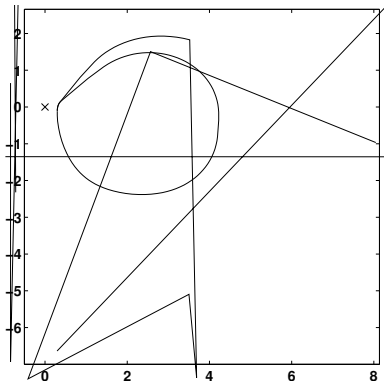

Fig. 5.8: The numerical range for $k = 10; 50; 100$ of A for the L-shaped domain.

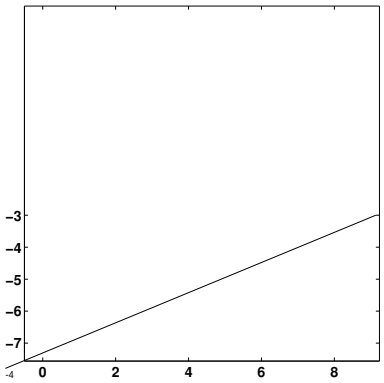

Fig. 5.9: The numerical range for $k = 10; 50; 100$ of A for a non-starshaped domain (\double-L").

If 0 is in the interior of the numerical range $W(A)$ for a resonance k_{res} then by continuity

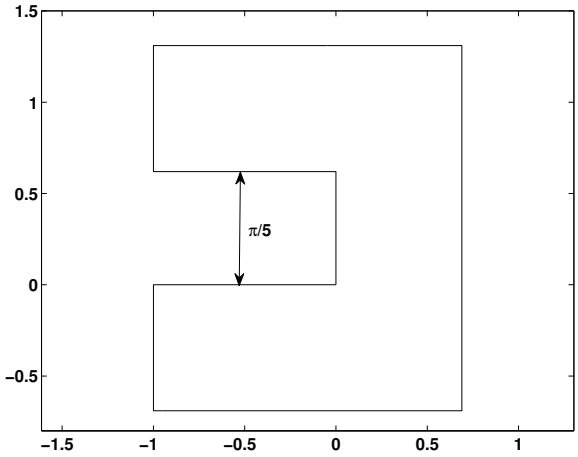

Fig. 5.10: A trapping domain. The open cavity has a width of =5.

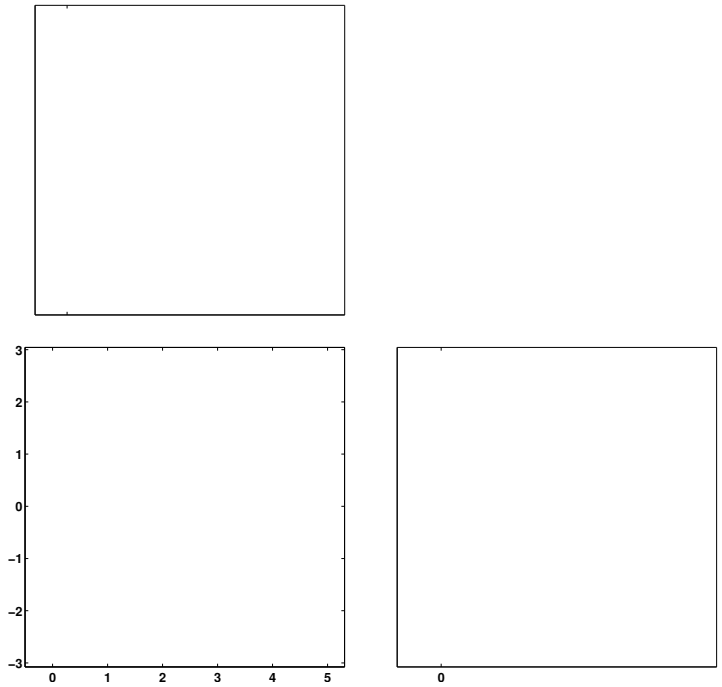

Fig. 5.11: The numerical range of A for the trapping domain from Figure 5.10 in the cases $k = 4; 5; 8; 10$.

fact, B_k can be analytically continued into $Im\{k\} < 0$ except for certain poles, and these are called the \resonances" or \scattering poles". When k is one of these scattering poles, there exists an outgoing solution of (1.5) *which is zero on @ , where a function v is called outgoing if*

$$v \quad C\frac{e^{ikr}}{r^{(d\ 1)=2}} \text{ as } r\ !\ 1;$$

where C depends only on the angular variables and d is the dimension. However outgoing solutions with k having negative imaginary part grow exponentially towards in nity and do not satisfy the Sommerfeld radiation condition (1.7)*.*

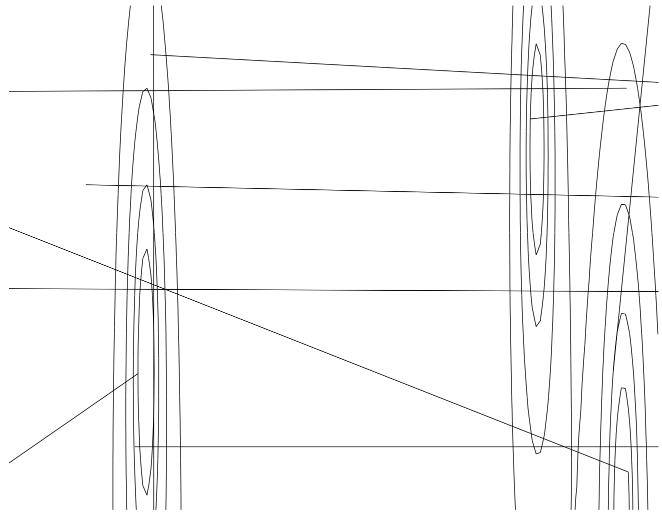

5.12

Fig. 5.12: Contour plot of $\log_{10}(\|A^{-1}_k\|)$ over a part of the complex plane. The dashed lines show ranges, where for k on the real axis the operator A is not coercive.

	Smooth	Polygonal
Convex	Circle {coercive, uniform in k	Square {coercive, uniform in k Equilateral triangle {coercive, uniform in k
Non-convex, star-shaped	Kite {coercive, uniform in k Inverted ellipse {coercive, not uniform in k	L-shaped {coercive, uniform in k
Non-star-shaped		Double-L {coercive, uniform in k Trapping {coercivity depends on k

Table 6.1: Summary of the numerical results on coercivity of the operator A on various domains for $k = 10; 50; 100$.

In a neighborhood of the positive real k axis, B_k can be expressed in terms of the boundary integral operator A^0_k, equation (2.1)*, as follows:*

$B_k = 2(D_k \quad i$ SeaSeSer4F614 9.u45(the)-346(op)-275.7034.902 2.822 -345(co)-28

of the operator to investigate coercivity on several interesting domains in two dimensions. The numerical results demonstrate that coercivity of the direct combined boundary integral operator A seems to hold uniformly on a wide range of domains. This is surprising since for standard domain based variational formulations of the underlying Helmholtz equation only a weaker Garding inequality, with k dependent perturbation term, holds [23]. Table 6.1 summarizes the results for the di erent domains. Coercivity seems to hold uniformly (with respect to the numerical accuracy of the results) and independently of the wavenumber for all considered domains apart from the inverted ellipse and the trapping domain. For the inverted ellipse it is not clear from the current results whether $! 0$ as $k ! 1$ or whether there exists a lower bound C, such that $C <$ for all su ciently large k. The trapping domain behaves very di erently from the other domains, and we saw that the boundary integral operator has resonances close to the real axis which helped explain why it is not coercive. This leads us to make the following conjecture:

Conjecture 6.1. *The combined boundary integral operator A is coercive on bounded domains for all wavenumbers k that are su ciently far away from a resonance.*

The fact that the trapping domain behaves so di erently from the other domains considered here is not surprising. Indeed, in scattering theory for the time dependent wave equation, the geometry of the domain, and in particular whether it is trapping or not, plays a key role [27]. Recall the de nition of \trapping" and \non-trapping" from the epilogue of [27]: consider all the rays starting in the exterior of inside some large ball of nite radius. Continue all the rays according to the law of re ection (angle of incidence equals angle of re ection) whenever they hit @ , until they nally leave the large ball. We call trapping if there are arbitrary long paths or closed paths of this kind; otherwise is non-trapping. (Note that there are subtleties associated with rays hitting the boundary at a tangent, and also for domains with non-smooth boundaries.)

The connection between whether a domain is trapping or not and the location of resonances is a classic problem: in the 1967 rst edition of [27], Lax and Philips conjectured that

1. for a non-trapping domain there are no resonances in a strip $fk : \mathrm{Im}fkg g$ for some constant > 0, and
2. for a trapping domain there is a sequence of resonances $fk_j g_{j=1}^{1}$ such that $\mathrm{Im}fk_j g ! 0$ as $j ! 1$.

The rst statement was proved to be correct in [31] and [30]; however examples of trapping domains for which there are no resonances in a strip below the real axis were given in [6], [24], and thus the second statement is incorrect. (More details about these results are given in [27, Epilogue].)

Returning to the question of coercivity, the result 1 above implies that for the inverted ellipse there are no resonances in a strip below the imaginary axis, lending support to the idea that coercivity is uniform for higher k. Combining Conjecture 6.1 with the result 1, leads to the following conjecture:

Conjecture 6.2. *The combined boundary integral operator A is coercive uniformly in k, for all su ciently large wavenumbers k*